## Title

Automating Scoliosis Measurements in Radiographic Studies with Machine Learning: Comparing Artificial Intelligence and Clinical Reports



**Journal**
Journal of Digital Imaging, 35(3)

**ISSN**
0897-1889

**Authors**
Ha, Audrey Y
Do, Bao H
Bartret, Adam L
et al.

**Publication Date**
2022-06-01

**DOI**
10.1007/s10278-022-00595-x

Peer reviewed

Journal of Digital Imaging (2022) 35:524–533
https://doi.org/10.1007/s10278-022-00595-x

ORIGINAL PAPER

# Automating Scoliosis Measurements in Radiographic Studies with Machine Learning: Comparing Artificial Intelligence and Clinical Reports

**Audrey Y. Ha[1] · Bao H. Do[1] · Adam L. Bartret[1] · Charles X. Fang[1] · Albert Hsiao[2] · Amelie M. Lutz[1] · Imon Banerjee[3] · Geoffrey M. Riley[1] · Daniel L. Rubin[1] · Kathryn J. Stevens[1] · Erin Wang[1] · Shannon Wang[1] · Christopher F. Beaulieu[1] · Brian Hurt[2]**

Received: 20 October 2021 / Revised: 20 January 2022 / Accepted: 24 January 2022 / Published online: 11 February 2022


**Abstract**
Scoliosis is a condition of abnormal lateral spinal curvature affecting an estimated 2 to 3% of the US population, or seven million people. The Cobb angle is the standard measurement of spinal curvature in scoliosis but is known to have high interobserver and intraobserver variability. Thus, the objective of this study was to build and validate a system for automatic quantitative evaluation of the Cobb angle and to compare AI generated and human reports in the clinical setting. After IRB was obtained, we retrospectively collected 2150 frontal view scoliosis radiographs at a tertiary referral center (January 1, 2019, to January 1, 2021, ≥ 16 years old, no hardware). The dataset was partitioned into 1505 train (70%), 215 validation (10%), and 430 test images (20%). All thoracic and lumbar vertebral bodies were segmented with bounding boxes, generating approximately 36,550 object annotations that were used to train a Faster R-CNN Resnet-101 object detection model. A controller algorithm was written to localize vertebral centroid coordinates and derive the Cobb properties (angle and endplate) of dominant and secondary curves. AI-derived Cobb angle measurements were compared to the clinical report measurements, and the Spearman rank-order demonstrated significant correlation (0.89, $p < 0.001$). Mean difference between AI and clinical report angle measurements was 7.34° (95% CI: 5.90–8.78°), which is similar to published literature (up to 10°). We demonstrate the feasibility of an AI system to automate measurement of level-by-level spinal angulation with performance comparable to radiologists.

**Keywords** Scoliosis · Cobb angle · Spine · Artificial intelligence · Deep learning · Convolutional neural network

## Introduction

Scoliosis, or the condition of abnormal spinal curvature, is caused by a wide array of etiologies. In the USA, over 600,000 office visits are made by scoliosis patients each year, and this condition impacts an estimated 2–3% of the US population, or seven million people [1]. Radiographs are the preferred imaging technique for scoliosis alignment, with cross-sectional imaging reserved for specific clinical scenarios. The most widely used measurement of spinal curvature is the Cobb angle, where greater than 10–12° of lateral curvature is considered abnormal. The Cobb angle was originally described by Cobb [2] and adopted as the standard measurement method by the Scoliosis Research Society, founded in 1966. To measure the Cobb angle, the most tilted superior and inferior vertebrae are identified (mathematically correlating to the inflection boundaries of a curve) and the angle between them is assessed, although the selected vertebrae may not be the exact locations of the curve inflections as endplate level is an anatomic landmark for improving reader consistency. The measurement of the Cobb angle is time consuming with high interobserver and intraobserver variability [3–6], and different selections of end-vertebrae are a major source of error [7]. The angle

✉ Brian Hurt
brhurt@health.ucsd.edu

1 Department of Radiology, Stanford University, 300 Pasteur Drive, Stanford, CA 94305, USA

2 Department of Radiology, University of California San Diego, 9300 Campus Point Drive, La Jolla, CA 92037, USA

3 Department of Radiology, Mayo Clinic, 5779 E Mayo Blvd, Phoenix, AZ 85054, USA

may vary up to 10° between observers, and reliability did not significantly improve even with the same end-vertebrae selected [3]. Thus, computer techniques have been suggested to improve consistency and accuracy.

Various researchers have applied mathematical modeling to standardize the measurement of the Cobb angle, including the Hough transformation developed by Zhang [8–10]. Anitha and Prabhu suggested identifying the horizontal inclinations of all vertebrae using active contouring and filtering [11, 12]. Different denoising techniques have been proposed with histogram equalization applied to enhance image contrast [13]. These pixel value heuristic based techniques are limited in generalizability. Recently, segmentation-based neural networks have also held promise for creating fully automatic systems to measure spinal curves [14, 15]. Although these methods are applicable for angle quantification, they require complex image processing steps including feature extraction, filtering, enhancement, and segmentation where user bias is still not eliminated. Additionally, secondary algorithms are still required to identify landmarks to extract the spinal axis and curve inflection boundaries in order to calculate scoliosis curve measurements.

Object detection convolutional neural networks (CNNs) can be used to identify visual objects and have been successfully implemented in radiology, such as detection of lumbar spinal stenosis [16] and intervertebral disks [17]. Potentially, object detection can identify vertebral bodies and localize their centroids to derive the spine axis and Cobb landmarks without the complex manual pre-processing and time-consuming annotation required of segmentation-based neural networks. Therefore, we hypothesize that a CNN-based object detection and measurement pipeline can be designed to automate the measurement and reporting of Cobb angles on scoliosis radiographs.

## Materials and Methods

### Scoliosis Radiographs

Institutional Review Board approval was obtained, and informed consent was waived for this retrospective, HIPAA compliant imaging review. Three thousand nine hundred fifty-seven sequential anteroposterior scoliosis radiographs from 2019 to 2021 were retrospectively collected from our tertiary care center institution. Two thousand four hundred two radiographs remained after excluding radiographs with hardware, and 2150 radiographs remained after excluding radiographs with inadequate exam quality, including poor soft tissue penetration, over-exposure, and image markups. Of patients, 59.9% were female and 40.1% of patients were male, with mean patient age 56.4 years ± 21.1 (standard deviation). Images were originally in Digital Imaging and Communications in Medicine (Dicom) format and were converted into de-identified Joint Photographic Experts Group (jpeg) files, with original resolution and default window and level settings. The data collection diagram and overall project architecture are shown in Fig. 1.

### Anatomic Localization for Thoracic and Lumbar Vertebrae

All 2150 radiographs were annotated using the LabelImg software by 3 investigators (A.Y.H., E.W., S.W.). A musculoskeletal attending with more than 10 years of experience (B.H.D.) reviewed and revised the annotations (36,550 objects). Rectangular bounding boxes encompassed the entirety of each vertebra, prioritizing the localization of the bounding box centroid to the vertebrae centroid for tilt and rotation. Annotations were then exported in standard Pascal VOC XML format.

A Faster R-CNN Resnet-101 model was implemented for vertebrae detection using the Object Detection API within the TensorFlow framework (Google, Mountain View, CA) [18]. We selected this model due to optimal efficiency and accuracy trade-offs after preliminary evaluation of multiple TensorFlow feature extraction models: Resnet-101, InceptionV2, and InceptionResnetV2 Atrous. Faster R-CNN is known for its shorter training time [19] and utilizes a region proposal network (RPN) to simultaneously predict potential object regions and the probability that each region is an object. Resnet-101 is a 101 layer-deep CNN utilizing shortcut connections between layers to enable deeper networks with preserved accuracy. Resnet-101 was used in the Faster R-CNN network to generate feature maps that were fed into the RPN (Fig. 2). After the RPN, a region of interest (RoI) pooling layer, upstream classifier, and bounding box regressor similar to that of Fast R-CNN were utilized to produce final bounding boxes and object predictions [20]. The Faster R-CNN Resnet-101 was initialized on pre-trained weights from the common objects in context (COCO) dataset [21], using transfer learning to accelerate weight convergence and reduce training requirements.

Training was performed on a workstation equipped with a NVIDIA Tesla V100 graphics card (NVIDIA, Santa Clara, CA). A training set consisting of 1505 (70%) radiographs was used to train the AI model to detect thoracic and lumbar vertebrae. Images were resized to a maximum dimension of 1024 pixels and train-time data augmentation was performed with random horizontal flips. Using a momentum optimizer [22] and an exponentially decaying learning rate starting at 0.0003, we trained the model until validation accuracy plateaued at approximately 100,000 steps.

After training and validation, the neural network could generate a list of bounding box coordinates for thoracic and lumbar vertebrae based on input images (Fig. 3a, b).

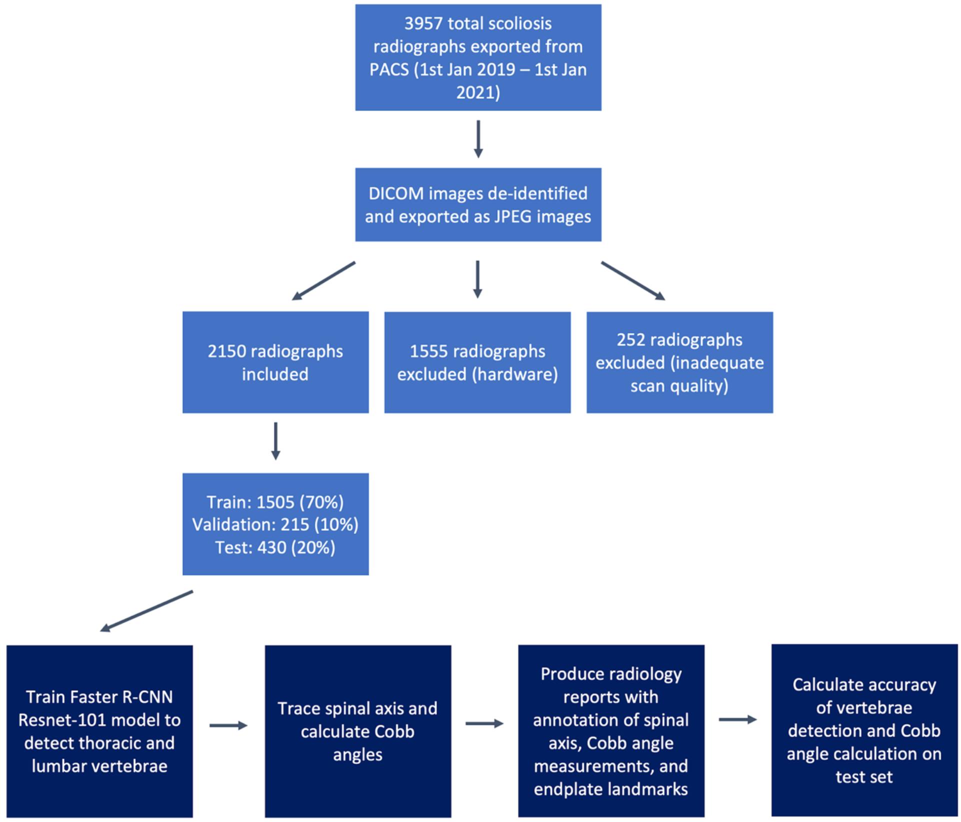


**Fig. 1** System pipeline for automatic measurement of the Cobb angle

Individual vertebral levels were assigned by their relative craniocaudal location within each class. Four hundred thirty (20%) sequential anteroposterior scoliosis radiographs excluding hardware were used to test the accuracy of thoracic and lumbar vertebrae detection. For each case, unique one-to-one mappings between annotated and predicted vertebral levels were computed using the highest intersection over union of predicted vertebrae for each annotated vertebrae. Given the mappings, the mean and 95% confidence interval were computed for intersection over union (IoU), Dice similarity coefficient, and the mean bounding box center point distance error (normalized by the annotated bounding box width and height). Additionally, the mean per-case percentage of vertebral levels correctly predicted was calculated by dividing the total number of mapped annotated vertebrae with the total number of annotated vertebrae.

## Cobb Angle Measurement

To compute Cobb angles, we developed an algorithm in Python employing spine localization (Fig. 4). The spine localization line is defined by a smoothed spline through the center points of predicted vertebrae bounding boxes, sorted craniocaudally, and filtered out if two center points are within a fixed number of pixels of one another. Lateral curvature angles are computed based on identifying apex, superior, and inferior vertebral bodies. Apex vertebrae are those bodies where the inflection of curvature at the center

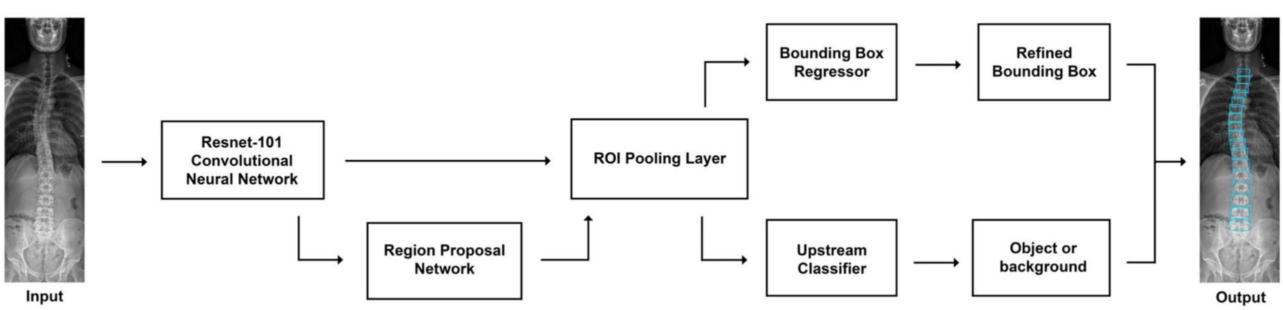


**Fig. 2** Faster R-CNN Resnet-101 model architecture

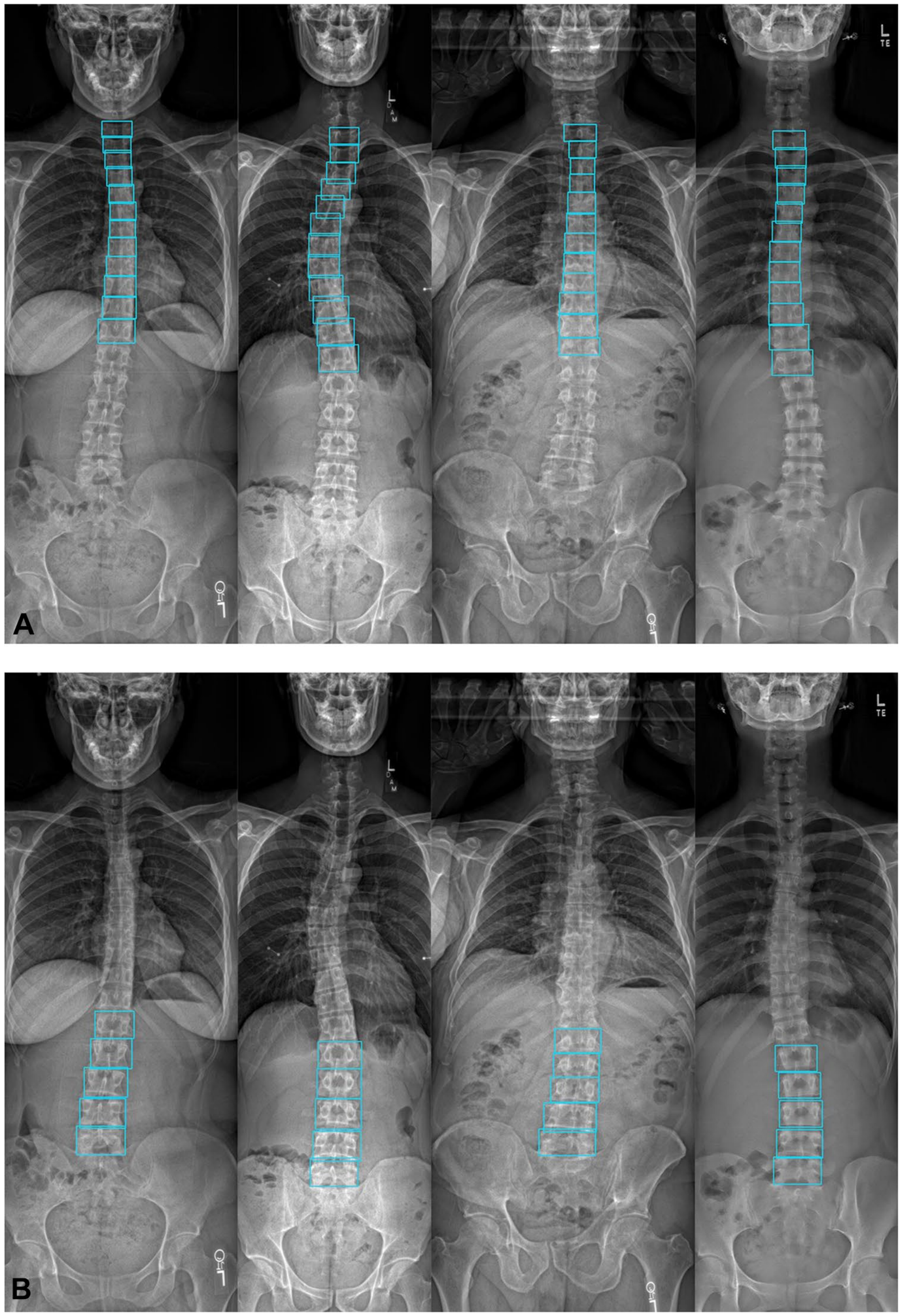


**Fig. 3** **a** Example thoracic vertebrae object detection output. **b** Example lumbar vertebrae object detection output

point is a local minima. The superior and inferior vertebral bodies associated with the apex are those where the inflection of curvature changes direction. The lateral curvature angle is calculated from the difference in slopes between superior and inferior body endplate points, which are estimated along the spine localization line based on their center point and bounding box craniocaudal coordinates. Figure 5 shows our Web app that receives a scoliosis radiograph as an input and then outputs a radiology report.

After running the object detection CNN on the separate test set (430 radiographs), the spine localization algorithm was used to extract Cobb angles from primary and secondary curves. These predictions were compared to Cobb angles computed from the manual bounding box annotations (3 reader team with expert adjudicator), and Cobb angle measurements manually extracted from clinical reports. Comparisons including the mean angle difference, Spearman rank-order correlation, bias, and standard deviation were computed.

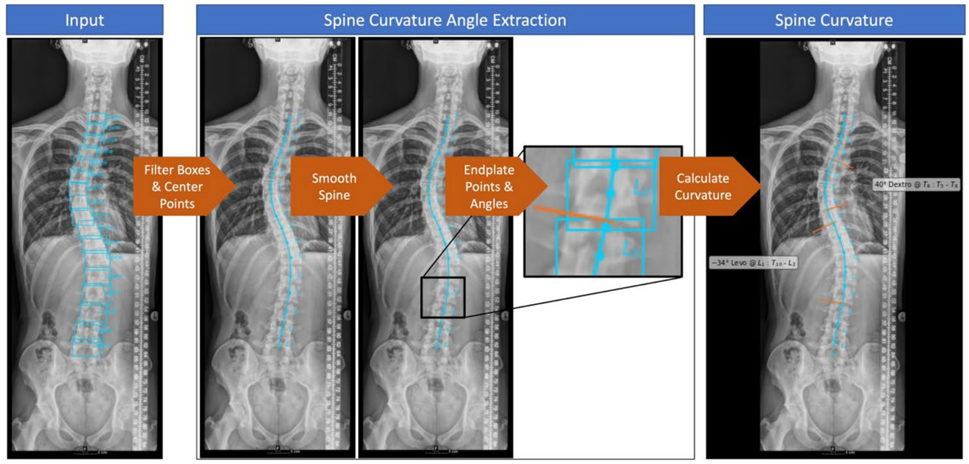


**Fig. 4** Calculating Cobb angles after vertebrae object detection

## Results

### Anatomic Localization for Thoracic and Lumbar Vertebrae

Using the 430 hold-out test cases, we calculated the IoU score, Dice similarity coefficient, normalized mean distance from the vertebrae box center, and percentage of vertebrae detected in order to obtain a comprehensive overview of object detection model accuracy. The test scores are presented in Table 1.

The IoU score for all vertebrae detection was 0.83 (95% CI: 0.82–0.83) and the Dice similarity coefficient was 0.90 (95% CI: 0.90–0.91), showing that our model achieved high success not only in detection, but also segmentation of each component of the vertebrae. Moreover, the tight confidence intervals show that the model is robust, as the performance variability is low for unseen test cases, even for challenging cases. The normalized mean distance from the vertebrae box center was 7.2% (95% CI: 6.8–7.9%), and the percentage of vertebrae detected was 0.98 (95% CI: 0.98–0.98), reflecting high accuracy for vertebral body object detection.

### Cobb Angle Measurement: Comparing Clinical Annotators and Object Detection CNN

Our test set included a total of 430 test radiographs (20% of dataset). In order to further compare the performance of clinical annotators and the object detection CNN, we ran the spine localization algorithm on [1] the human annotators' bounding boxes and [2] the object detection CNN's bounding boxes. The spine localization algorithm found 312 Cobb angles in [1] and [2], and the angle values were compared. This yielded a mean absolute angle difference was 5.46 degrees (95% CI: 4.60–6.29°), a Spearman rank-order correlation of 0.95 ($p < 0.001$), and a proportional bias and standard deviation of $-0.39 \pm 9.38°$ (Fig. 6a).

### Cobb Angle Measurement: Comparing Clinical Reports and Object Detection CNN

Out of the 430 test radiographs, 56 of the radiographs had clinical reports containing at least one numerical Cobb angle value. Three cases were removed since the spine localization algorithm did not identify one of the Cobb angles. In the remaining 53 reports, a total of 70 Cobb angle values were matched and compared to those computed by the spine localization algorithm. These measurements had a mean absolute angle difference of 7.34° (95% CI: 5.90–8.78°), a Spearman rank-order correlation of 0.89 ($p < 0.001$), and a proportional bias and standard deviation of $0.00 \pm 9.62°$ (Fig. 6b).

## Discussion

We demonstrated that a deep learning model trained on scoliosis radiographs could automatically measure the Cobb angle with high accuracy. To our knowledge, this study is the first to evaluate use of a recurrent neural network in conjunction with a CNN to quantify spinal curves in a radiographic image. The task of measuring a Cobb angle is relatively straightforward for a trained physician but can be time consuming and a source of both interobserver and intraobserver variation. In clinical practice, errors for manual Cobb angle measurement can often occur during selection of the most tilted vertebrae and manual drawing of a line across the endplates. As a result, automated detection and measurement of scoliosis curvature was recently identified by the ACR Data Science Institute as a use case with great promise for clinical practice, where the applications of artificial intelligence offer clinical and economic value [23].

AI neural networks have recently been introduced for fully automated Cobb angle measurement systems [24]. Although U-net or segmentation based neural networks may allow for the identification of spinal curve inflections to


**Fig. 5** Web app for automatic measurement of the Cobb angle

**Table 1** Vertebrae object detection accuracy

| Test | Score |
|---|---|
| Intersection over union (IoU) | 0.83 (95% CI: 0.82–0.83) |
| Dice similarity coefficient | 0.90 (95% CI: 0.90–0.91) |
| Normalized mean distance from center | 7.2% (95% CI: 6.8–7.9%) |
| Percentage of vertebrae predicted | 0.98 (95% CI: 0.98–0.98) |

generate quantification of the curve, they are often dependent on heavy manual preprocessing for training. We utilized object detection based CNNs that are more efficient to train, robust to variability, and have been previously used for medical diagnosis tasks such as detecting lumbar spinal stenosis [16] and intervertebral disks [17].

Using 1505 scoliosis radiographs, we trained a Faster R-CNN Resnet-101 model to automatically detect vertebral bodies, with an IoU of 0.83 (95% CI: 0.82–0.83) and Dice similarity coefficient of 0.90 (95% CI: 0.90–0.91). Sun et al. in 2019 utilized U-nets and obtained an IoU of $0.91 \pm 0.05$ (SD) for vertebrae segmentation [14]; Peng et al. in 2021 obtained a Dice similarity coefficient of $0.94 \pm 0.03$ (SD) using a vertebral body segmentation approach [15]. However, clinical interpretation of these metrics and their clinical significance is limited as there is no direct link between these metrics alone, since they are only the initial anatomic localization steps. Deriving Cobb angle measurements additionally requires a controller algorithm to compute angles between identified inflections.

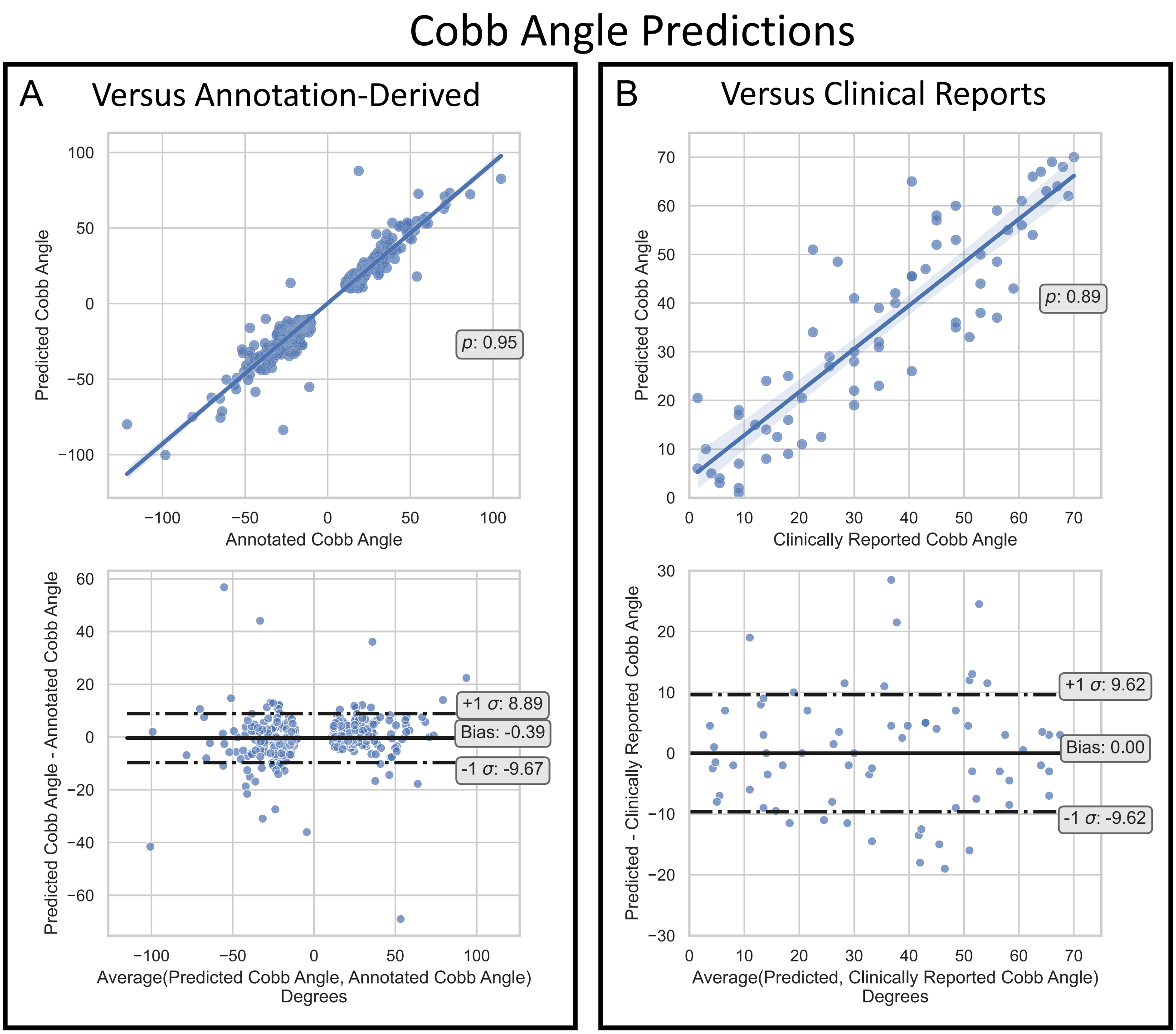


**Fig. 6** **a** Comparison of Cobb angle measurements derived from bounding box annotations and object detection CNN. **b** Comparison of Cobb angle measurements derived from clinical reports and object detection CNN

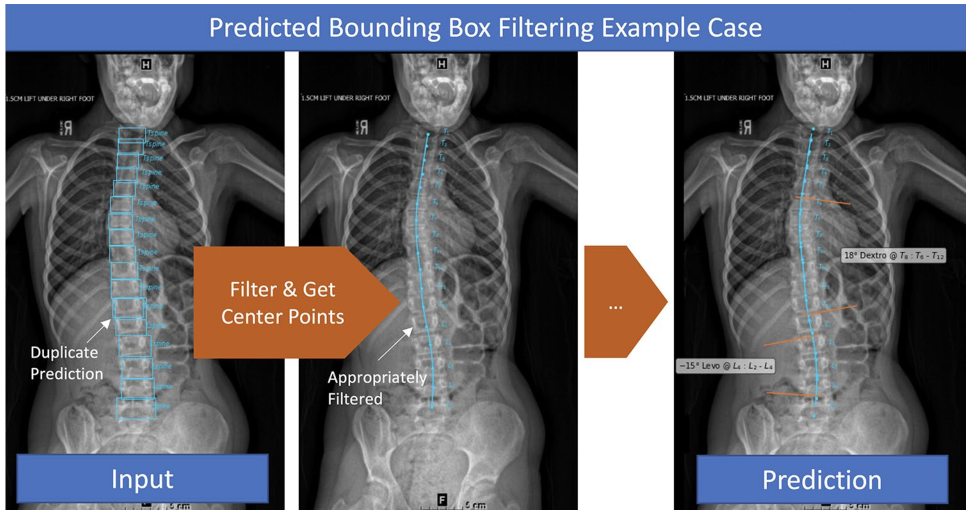


**Fig. 7** Example where duplicate bounding box prediction was filtered and Cobb angle was successfully calculated

To evaluate clinical utility, we wrote a spine localization algorithm to calculate Cobb angles from vertebral body bounding boxes. On a relatively large set of radiographs, our results demonstrate a high and significant correlation (0.95, $p<0.001$) between Cobb angles calculated from manually annotated bounding boxes and Cobb angles calculated from the object detection CNN's bounding boxes, suggesting reliable performance with our clinical annotators.

Similarly, the spine localization algorithm's Cobb angle measurements strongly and significantly correlated (0.89, $p<0.001$) with Cobb angle measurements from the clinical reports. Prior works from Sun et al. in 2019 demonstrated a Spearman rank-order correlation of 0.89 ($p=0.000$) when comparing an expert reader's Cobb angle measurements to AI, and Peng et al. in 2021 obtained Spearman rank-order correlations of 0.94 and 0.93 when comparing two experts to the computer algorithm. Our results reflect similar reliability to previous studies that used segmentation based neural networks, which require more manual preprocessing and annotation time.

While the system performed well overall, individual case inspection offers insight into some of its strengths and limitations. Figure 7 demonstrates a case where there was a duplicate bounding box prediction, and our algorithm successfully filtered out the duplicate box and calculated the Cobb angle. However, Fig. 8 demonstrates a case where the Cobb angle was not calculated due to a missing predicted bounding box. There are various opportunities for improvement and fine-tuning of the R-CNN model as our dataset consisted of non-hardware cases. Training the object detection model on a larger volume of studies and accounting for differences in hardware, obesity, and image quality may improve the model's clinical application.

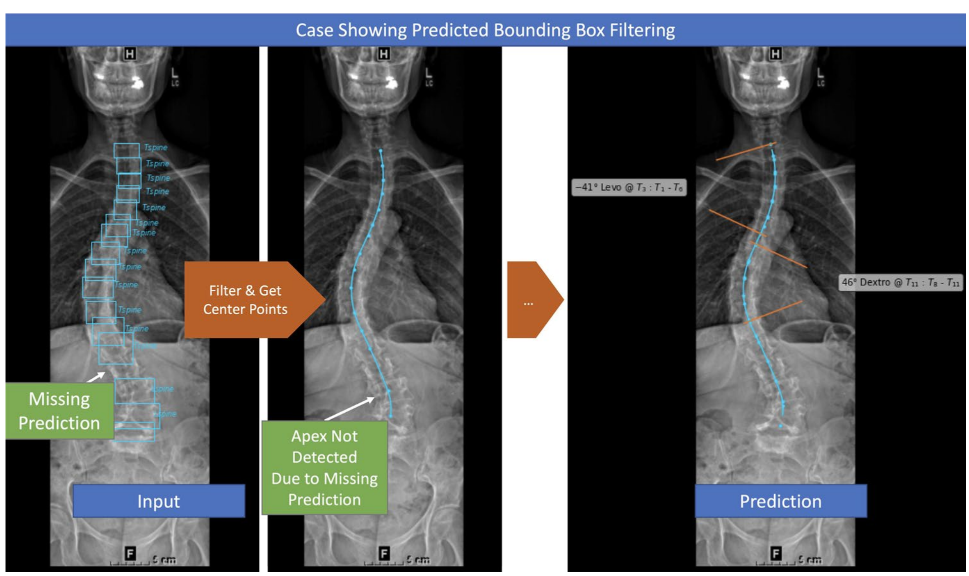


**Fig. 8** Example where Cobb angle was not calculated due to missing predicted bounding box

The Python algorithm that calculated the Cobb angle offers numerous opportunities for editing parameters to customize physician measurement preferences, potentially for providers, such as editing the thresholds on reported curves (minimum angle, number of vertebral bodies, level of vertebral bodies). By presenting the annotated image to the interpreting physician, occasional discrepant curves can be refined manually. The 70 Cobb angles from the 53 clinical reports represent a variety of observers, accounting for interobserver variability. The average difference between the AI and clinical report measurements was 7.34 degrees (95% CI: 5.90–8.78°), similar to the error for human observers, which was up to 10° (3, 4). Future steps include comparing additional readers to the algorithm's Cobb angle measurements.

As a next step for efficient workflow, a work-in-progress at our institution is incorporating the AI system into PACS with a display of the annotated image along with the original image and a pre-drafted report in the dictation system. Currently, we have developed a publicly available Web application that uses our object detection neural network and spine localization algorithm to assess scoliosis radiographs.

We developed and validated a system to automate evaluation and quantification of the spinal curve, tracing the spine and extracting Cobb angles by identifying upper and lower Cobb landmarks. In our test set, the system performed with a high IoU, Dice similarity coefficient, and Spearman rank-order correlation value, with promising Cobb angle measurement performance relative to clinical reports in our limited study. With additional training and incorporation in workflow, this methodology is promising as an approach to build fully automated systems for efficient, reliable, and consistent Cobb angle measurements in clinical practice.

**Author Contribution** Study supervision and guarantor of the article: Brian Hurt. Analysis and control of the data: Audrey Y. Ha, Bao H. Do, Adam L. Bartret, Charles X. Fang, Erin Wang, Shannon Wang, Brian Hurt. Data interpretation, review and revision of the manuscript: all authors.

**Code Availability** Our end-to-end AI system is part of a freely available web application: https://stanford.edu/~baodo/scoliosisai.htm.

## Declarations

**Ethics Approval** We retrospectively obtained all scoliosis radiographs from our tertiary care center under Institutional Review Board approval, and informed consent was waived for this HIPAA compliant imaging review.

**Conflict of Interest** There are no conflicts of interests that pertain specifically to this work. However, some of the authors are consultants for the medical industry and received grants not related to this study. Albert Hsiao is a founder and consultant for Arterys Inc. and receives grant support from GE Healthcare, Bayer AG, and the American Roentgen Ray Society as an ARRS Scholar, unrelated to this study. Brian Hurt provides consulting services to Imidex Inc unrelated to this study, and supported by the NIH T32EB005970. Amelie M. Lutz receives research funding from GE Healthcare and material support from Bracco Diagnostics Inc. for projects not related to this study. Kathryn J. Stevens receives research funding from GE Healthcare for projects not related to this study.

## References

1. National Scoliosis Foundation [August 30, 2020]. NSF is a patient-led nonprofit organization dedicated to helping children, parents, adults, and health-care providers to understand the complexities of spinal deformities such as scoliosis.]. Available from: https://www.scoliosis.org/info.php
2. Cobb JR. Outline for the study of scoliosis. American Academy of Orthopaedic Surgeons. Instr Course Lect. 1948;5:261-75.
3. Carman DL, Browne RH, Birch JG. Measurement of scoliosis and kyphosis radiographs. Intraobserver and interobserver variation. J Bone Joint Surg Am. 1990;72(3):328–33. Epub 1990/03/01. PubMed PMID: 2312528.
4. Loder RT, Urquhart A, Steen H, Graziano G, Hensinger RN, Schlesinger A, et al. Variability in Cobb angle measurements in children with congenital scoliosis. J Bone Joint Surg Br. 1995;77(5):768-70. Epub 1995/09/01. PubMed PMID: 7559707.
5. Morrissy RT, Goldsmith GS, Hall EC, Kehl D, Cowie GH. Measurement of the Cobb angle on radiographs of patients who have scoliosis. Evaluation of intrinsic error. J Bone Joint Surg Am. 1990;72(3):320–7. Epub 1990/03/01. PubMed PMID: 2312527.
6. Pruijs JE, Hageman MA, Keessen W, van der Meer R, van Wieringen JC. Variation in Cobb angle measurements in scoliosis. Skeletal Radiol. 1994;23(7):517–20. Epub 1994/10/01. https://doi.org/10.1007/BF00223081. PubMed PMID: 7824978.
7. Gstoettner M, Sekyra K, Walochnik N, Winter P, Wachter R, Bach CM. Inter- and intraobserver reliability assessment of the Cobb angle: manual versus digital measurement tools. Eur Spine J. 2007;16(10):1587–92. Epub 2007/06/06. https://doi.org/10.1007/s00586-007-0401-3. PubMed PMID: 17549526; PubMed Central PMCID: PMCPMC2078306.
8. Zhang J, Lou E, Hill DL, Raso JV, Wang Y, Le LH, et al. Computer-aided assessment of scoliosis on posteroanterior radiographs. Med Biol Eng Comput. 2010;48(2):185–95. Epub 2009/12/17. https://doi.org/10.1007/s11517-009-0556-7. PubMed PMID: 20012376.
9. Zhang J, Lou E, Le LH, Hill DL, Raso JV, Wang Y. Automatic Cobb measurement of scoliosis based on fuzzy Hough Transform with vertebral shape prior. J Digit Imaging. 2009;22(5):463–72. Epub 2008/06/03. https://doi.org/10.1007/s10278-008-9127-y. PubMed PMID: 18516643; PubMed Central PMCID: PMCPMC3043716.
10. Zhang J, Lou E, Shi X, Wang Y, Hill DL, Raso JV, et al. A computer-aided Cobb angle measurement method and its reliability. J Spinal Disord Tech. 2010;23(6):383–7. Epub 2010/02/04. https://doi.org/10.1097/BSD.0b013e3181bb9a3c. PubMed PMID: 20124919.
11. Anitha H, Prabhu GK, Karunakar AK. Reliable and reproducible classification system for scoliotic radiograph using image processing techniques. J Med Syst. 2014;38(11):124. Epub 2014/09/28. https://doi.org/10.1007/s10916-014-0124-z. PubMed PMID: 25261171.

12. Anitha H, Prabhu GK. Automatic quantification of spinal curvature in scoliotic radiograph using image processing. J Med Syst. 2012;36(3):1943–51. Epub 2011/01/27. https://doi.org/10.1007/s10916-011-9654-9. PubMed PMID: 21267773.
13. Mukherjee J, Kundu R, Chakrabarti A. Variability of Cobb Angle Measurement from Digital X-ray Image Based on Different Denoising Techniques. International Journal of Biomedical Engineering and Technology, Inderscience. 2014;16. https://doi.org/10.1504/IJBET.2014.065656.
14. Horng MH, Kuok CP, Fu MJ, Lin CJ, Sun YN. Cobb Angle Measurement of Spine from X-Ray Images Using Convolutional Neural Network. Comput Math Methods Med. 2019;2019:6357171. Epub 2019/04/19. https://doi.org/10.1155/2019/6357171. PubMed PMID: 30996731; PubMed Central PMCID: PMCPMC6399566.
15. Liu J, Yuan C, Sun X, Sun L, Dong H, Peng Y. The measurement of Cobb angle based on spine X-ray images using multi-scale convolutional neural network. Physical and Engineering Sciences in Medicine. 2021;44(3):809-21. doi: https://doi.org/10.1007/s13246-021-01032-z.
16. Hallinan JTPD, Zhu L, Yang K, Makmur A, Algazwi DAR, Thian YL, et al. Deep Learning Model for Automated Detection and Classification of Central Canal, Lateral Recess, and Neural Foraminal Stenosis at Lumbar Spine MRI. Radiology. 2021:204289. https://doi.org/10.1148/radiol.2021204289.
17. Sa R, Owens W, Wiegand R, Studin M, Capoferri D, Barooha K, et al., editors. Intervertebral disc detection in X-ray images using faster R-CNN. 2017 39th Annual International Conference of the IEEE Engineering in Medicine and Biology Society (EMBC). 11–15 July 2017.
18. Abadi Mi, Barham P, Chen J, Chen Z, Davis A, Dean J, et al. TensorFlow: A system for large-scale machine learning. arXiv pre-print server. 2016. arxiv:1605.08695
19. Ren S, He K, Girshick R, Sun J. Faster R-CNN: Towards Real-Time Object Detection with Region Proposal Networks. IEEE Trans Pattern Anal Mach Intell. 2017;39(6):1137–49. Epub 2016/06/14. https://doi.org/10.1109/tpami.2016.2577031. PubMed PMID: 27295650.
20. Girshick R. Fast R-CNN. arXiv pre-print server. 2015. arxiv:1504.08083.
21. Lin T-Y, Maire M, Belongie S, Hays J, Perona P, Ramanan D, et al. editors. Microsoft COCO: Common Objects in Context. Computer Vision – ECCV 2014. Cham: Springer International Publishing.
22. Qian N. On the momentum term in gradient descent learning algorithms. Neural Netw. 1999;12(1):145–51. Epub 2003/03/29. https://doi.org/10.1016/s0893-6080(98)00116-6. PubMed PMID: 12662723.
23. Allen B. AI Use Cases with Clinical Promise 2018 [March 6, 2021]. Available from: https://www.acrdsi.org/DSIBlog/2018/10/16/21/55/AI-Use-Cases-with-Clinical-Promise.
24. Galbusera F, Niemeyer F, Wilke HJ, Bassani T, Casaroli G, Anania C, et al. Fully automated radiological analysis of spinal disorders and deformities: a deep learning approach. Eur Spine J. 2019;28(5):951–60. Epub 2019/03/14. https://doi.org/10.1007/s00586-019-05944-z. PubMed PMID: 30864061.